Efficient Langevin simulation of coupled classical fields and fermions

Kipton Barros[1,*] and Yasuyuki Kato[1,2]

[1]*Theoretical Division and CNLS, Los Alamos National Laboratory, Los Alamos, New Mexico 87545, USA*

[2]*RIKEN Center for Emergent Matter Science (CEMS), Wako, Saitama 351-0198, Japan*

(Received 11 March 2013; revised manuscript received 2 July 2013; published 2 December 2013)

We introduce an efficient Langevin method to study bilinear fermionic Hamiltonians interacting with classical fields. Our approach is orders of magnitude faster than previous methods when applied to very large systems with high accuracy requirements. To demonstrate the method, we study complex noncoplanar chiral spin textures on the triangular Kondo lattice model. We also explore nonequilibrium mesoscale physics such as chiral domain coarsening and $\mathbb{Z}_2$ vortex annihilation.

DOI: 10.1103/PhysRevB.88.235101 PACS number(s): 75.30.Mb, 05.10.Ln, 71.15.−m, 71.27.+a

Lattice models of fermions interacting with classical fields encompass a wide range of physics. Popular examples in condensed matter include Kondo lattice (KL) models of itinerant electrons interacting with localized magnetic moments,[1] Falicov-Kimball models of metal-insulator transitions in rare-earth materials,[2] and Bogoliubov-De Gennes equations for superconductivity.[3] The Hubbard-Stratonovich transformation is another path to obtaining bilinear fermionic systems coupled to an auxiliary classical field.[4,5] This broad class of models poses a notoriously difficult numerical challenge: Monte Carlo (MC) sampling of the classical field requires *repeated* diagonalization of the single-particle fermion matrix.

In the context of KL models, several MC methods have been developed to more efficiently sample the classical field of local magnetic moments.[6–11] These methods have largely been applied to the ferromagnetic transition at large coupling.[12–14] This transition is relatively easy to study using moderate temperatures and small system sizes.

Recent interest has shifted to exotic spin textures which occur at small to moderate couplings. Skyrmion lattices have recently been observed with spatial modulations up to 0.1 μm.[15,16] Chiral textures lead to an anomalous Hall effect associated with huge ($\sim 10^5$ T) effective magnetic fields, as predicted in the KL model on a triangular lattice[17,18] and experimentally observed in $Pr_2Ir_2O_7$[19] and UCu_5.[20] Compared to ferromagnetism, these spin textures are very challenging to simulate. High precision and large system sizes are needed to capture the effective long-range physics at low temperatures.

In this paper we introduce an efficient Langevin method that updates the entire classical field at a cost that scales *linearly* with system size. The core of our method is the estimation of Langevin forces, which we obtain by a nontrivial gradient transformation[21] of the kernel polynomial method (KPM).[22,23] We demonstrate orders of magnitude efficiency gains over previous methods in applications to very large systems with high accuracy requirements. In studies of the triangular KL model, we use our method to find equilibrium phases and nonequilibrium effects such as chiral domain coarsening and $\mathbb{Z}_2$ vortex dynamics.

Our method applies to a general bilinear fermionic Hamiltonian coupled to continuous, classical degrees of freedom ϕ,

$$\mathcal{H} = \sum_{ij} c_i^\dagger A_{ij}[\phi] c_j, \tag{1}$$

with sparse matrix A. We work at fixed temperature T (in units with $k_B = 1$) and chemical potential μ. The partition function is a trace over classical and fermionic degrees of freedom, $Z = \mathrm{Tr}_\phi \mathrm{Tr}_c \exp[-(\mathcal{H} - \mu \sum_i c_i^\dagger c_i)/T]$. Evaluating the fermionic trace yields $Z = \mathrm{Tr}_\phi\, e^{-F/T}$, where

$$F[\phi] = \int \rho(\epsilon) f(\epsilon)\, \mathrm{d}\epsilon$$

is the effective energy functional of classical field ϕ, $\rho(\epsilon) = \sum_\nu \delta(\epsilon - \epsilon_\nu[\phi])$ is the density of states of $A[\phi]$, and $f(\epsilon) = -T \log[1 + e^{-(\epsilon-\mu)/T}]$. The fermion mediated effective energy $F[\phi]$ may be long range and many body.

A key difficulty in MC sampling the classical field is calculating ΔF in response to changes in ϕ. KPM begins by approximating the density of states as a Chebyshev polynomial series,[22–24]

$$\rho(\epsilon) \approx \frac{1}{\pi\sqrt{1-\epsilon^2}} \sum_{m=0}^{M-1} (2 - \delta_{0,m}) g_m \mu_m T_m(\epsilon).$$

The expansion is valid when all eigenvalues of A have magnitude less than one; for typical lattice models, simple shifting and rescaling of the Hamiltonian is necessary.[23] The Chebyshev series can be related to the Fourier cosine series via the trigonometric representation of Chebyshev polynomials, $T_m(x) = \cos(m \arccos x)$. Like a Fourier series, direct truncation (i.e., setting $g_m = 1$) leads to unwanted Gibbs oscillations in regions where $\rho(\epsilon)$ rapidly varies. To optimally eliminate these artifacts, we apply the damping factors corresponding to the Jackson kernel,[23,25,26]

$$g_m = \frac{(M-m+1)\cos\frac{\pi m}{M+1} + \sin\frac{\pi m}{M+1}\cot\frac{\pi}{M+1}}{M+1}.$$

The heart of KPM is efficient estimation of the Chebyshev moments $\mu_m = \mathrm{Tr}\, T_m(A)$. The trace may be expressed as an ensemble average $\mu_m = \langle r^\dagger T_m(A) r\rangle$ over random column vectors r with elements that satisfy $\langle r_i^* r_j\rangle = \delta_{ij}$. The single random vector approximation $\mu_m \approx r^\dagger T_m(A) r$ may be sufficient.[22] A recursive procedure to estimate μ_m follows from the definition of Chebyshev polynomials,

$$T_m(A) = \begin{cases} 1 & m = 0 \\ A & m = 1 \\ 2AT_{m-1}(A) - T_{m-2}(A) & m > 1 \end{cases}.$$

Combining these results, we obtain the complete KPM procedure to estimate $F[\phi]$,

$$F = \sum_{m=0}^{M-1} C_m \mu_m \tag{2}$$

$$\mu_m = r^\dagger \cdot \alpha_m \tag{3}$$

$$\alpha_m = \begin{cases} r & m = 0 \\ Ar & m = 1 \\ 2A\alpha_{m-1} - \alpha_{m-2} & m > 1 \end{cases}, \tag{4}$$

involving only matrix-vector products. When A is a sparse matrix with $\mathcal{O}(N)$ elements, this recursive procedure requires only $\mathcal{O}(MN)$ operations. The coefficients

$$C_m = \frac{1}{\pi}(2 - \delta_{0,m}) g_m \int_{-1}^{1} \frac{T_m(\epsilon) f(\epsilon)}{\sqrt{1-\epsilon^2}} \mathrm{d}\epsilon$$

are independent of A and may be efficiently evaluated using Chebyshev-Gauss quadrature.[23,27] We draw complex elements r_i from the uniform distribution $|r_i|^2 = 1$.[28]

There are two independent sources of error in the KPM estimate of $F[\phi]$: series truncation at order $M-1$, and stochastic estimation by averaging over finitely many random vectors r. Both are well controlled and will be discussed.

In this paper we go beyond standard KPM by *transforming* it to a procedure more suitable for sampling classical fields $\{\phi\}$ from the Boltzmann distribution, $P[\phi] \propto e^{-F[\phi]/T}$. We begin with the overdamped Langevin equation in discretized form

$$\phi_i(t + \Delta t) - \phi_i(t) = -\Delta t \frac{\partial F}{\partial \phi_i} + \sqrt{2T\Delta t}\eta_i(t), \tag{5}$$

where $\eta_i(t)$ are uncorrelated Gaussian random variables with unit variance and t is Langevin time. In this approach we simultaneously update all components ϕ_i. Efficient and accurate estimation of $\partial F/\partial \phi_i$ is crucial. We exclude inertial terms from the Langevin equation because they would amplify errors in the gradient estimate.

The technique of automatic differentiation with "reverse accumulation"[21] ensures that, by careful application of the chain rule, we can transform the KPM procedure to estimate F, Eqs. (2)–(4), into one that estimates $\partial F/\partial \phi_i$ for all i at the *same cost*. We perform this transformation analytically and state only the final recursive procedure, now descending in the index m,

$$\frac{\partial F}{\partial A_{ij}} = \beta_{0;i}\alpha_{0;j} + 2\sum_{m=1}^{M-2} \beta_{m;i}\alpha_{m;j}. \tag{6}$$

$$\beta_m = \begin{cases} 0 & m \geqslant M-1 \\ C_{m+1}r^\dagger + 2\beta_{m+1}A - \beta_{m+2} & m < M-1 \end{cases}. \tag{7}$$

The desired gradient is obtained by the chain rule,

$$\partial F/\partial \phi_i = \sum_{kl} (\partial F/\partial A_{kl})(\partial A_{kl}/\partial \phi_i).$$

The sequence of vectors α_m is the same as in the original KPM, but is required here in reverse order. We recalculate them as needed using $\alpha_m = 2A\alpha_{m+1} - \alpha_{m+2}$. The recursion begins with α_{M-1} and α_{M-2}, which are available at the end of the original KPM procedure.

The recursive procedure of Eqs. (6) and (7) to estimate *all* Langevin forces $\partial F/\partial \phi_i$ is our main result. Like the original KPM procedure, only $\mathcal{O}(M)$ sparse matrix-vector multiplications are required per random vector.

TABLE I. Several proposed methods for sampling a classical field coupled to fermions. In local MC (LMC) methods, a full system sweep corresponds to a local Metropolis MC update of each spin. In dynamical methods, a sweep is taken to be one unit of integration time. See the text for discussion.

Method	Sweep cost
LMC with direct diagonalization	$\mathcal{O}(N^3 \times N)$
LMC with low-rank rediagonalization (Ref. 10)	$\mathcal{O}(N^2 \times N)$
LMC with Green function KPM (Ref. 11)	$\mathcal{O}(NM \times N)$
LMC with truncated KPM (Refs. 7–9)	$\mathcal{O}(M^{d+1} \times N)$
Molecular dynamics with exact KPM (Ref. 29)	$\mathcal{O}(N^2 M/\Delta t)$
Hybrid MC with "perfect action" (Ref. 6)	$\mathcal{O}(\frac{N\tilde{M}^2 L_\tau f_{\mathrm{inv}} f_{\mathrm{mc}}}{\Delta t})$
Our KPM based Langevin method	$\mathcal{O}(NM/z)$

The gradient calculation also inherits the approximation errors of KPM, controlled by the truncation order M of the Chebyshev series and the dynamical stochastic error $z \equiv \Delta t/Q$, where Q is the number of of KPM random vectors used per time step. The KPM estimated density of states $\rho(\epsilon)$ is resolved to order $\Delta\epsilon/M$, where $\Delta\epsilon = \epsilon_{\max} - \epsilon_{\min}$ is the span of extremal eigenvalues. The parameter M should be large enough to resolve the physically relevant features of the density of states. The stochastic error $z > 0$ acts like an additional noise term in the Langevin dynamics, effectively adjusting $T \to T + \Delta T_{\mathrm{eff}}$. For matrices of the form $A(J\phi)$, where $J \ll 1$, the estimate of the force term $\Delta t(\partial F/\partial \phi_i)$ includes a stochastic error that scales as $\Delta t J/\sqrt{Q} = \sqrt{J^2 z \Delta t}$. Comparison with Eq. (5) suggests modeling this error as an additional noise term with a temperature that scales as $\Delta T_{\mathrm{eff}} \sim J^2 z$. The parameter z should be chosen such that $\Delta T_{\mathrm{eff}} \ll T$ for the smallest relevant temperature scale T.

Our method remains efficient at high accuracy: The cost to integrate the Langevin equation one unit of time is $\mathcal{O}(NM/z)$. Table I compares our method to several previous ones. To compare to Metropolis MC with local updates, we assume that one unit of Langevin integration time is roughly equivalent to a full MC sweep in which all N lattice sites are visited. Trial MC changes $\Delta\phi_i$ are accepted with a probability that depends on the change in energy ΔF. Brute force exact diagonalization of matrix A requires $\mathcal{O}(N^3)$ operations, and a full MC sweep costs $\mathcal{O}(N^4)$. This may be reduced to $\mathcal{O}(N^3)$ by tracking the response of the spectrum to low-rank changes in A.[10,30] Further acceleration is possible with KPM approximation. A nonstochastic Green's function method reduces the cost of a full MC sweep to $\mathcal{O}(MN^2)$.[11] In an alternative approach, if A contains only local coupling in d dimensions, a full MC sweep may be performed at cost $\mathcal{O}(M^{d+1}N)$.[8] In simulations presented below with $d = 2$, $N = 100^2$, $M = 1000$, and $z = 0.02$, our Langevin approach outperforms these local MC methods by two orders of magnitude or more.

Other dynamical methods have been proposed which, like our Langevin approach, update the entire classical field at each integration time step Δt. In atomic simulations, the tight-binding method may be used to approximate interatomic forces.[31] Cast in the form of Eq. (1), ϕ represents the positions of atomic nuclei which evolve classically according

to Newton's equations. A nonstochastic version of KPM has been applied to estimate the tight-binding forces.[29] Each integration time step costs $\mathcal{O}(N^2M)$.[32] Our Langevin approach is similar to that of Ref. 29, except we use stochastic force estimation to obtain linear scaling in N, and overdamped dynamics to prevent the accumulation of stochastic error.

A different strategy is employed by hybrid Monte-Carlo methods,[33,34] where the dynamics of ϕ is derived from an *approximate* action, and corrected with an MC accept/reject step. The standard field-theoretic approach uses a Suzuki-Trotter expansion to approximate the fermionic trace as an integral over L_τ Grassmann variables (with $\Delta\tau \sim 1/L_\tau$ the discretization length in the Trotter direction). The representation becomes exact in the continuum limit, $L_\tau \to \infty$. A subsequent transformation yields an integral over L_τ complex-valued pseudofermionic variables. The approximate action and its derivatives, given as a function of the pseudofermions, can be used to dynamically sample the classical field ϕ. Alonso *et al*. demonstrated that the path integral representation can be made exact for any *finite* L_τ provided that one uses a "perfect" action based upon $\exp(A/L_\tau T)$, the exponential of the single particle matrix.[6] A Legendre polynomial expansion, truncated at order $\tilde{M}$, may be used to estimate the perfect action and its relevant derivatives. The cost to integrate ϕ one dynamical time step scales like $\mathcal{O}(N\tilde{M}^2 L_\tau f_{\rm inv})$. The factor $f_{\rm inv}$ represents the cost of solving linear equations involving $\exp(A/L_\tau T)$, which become increasingly ill conditioned with decreasing $L_\tau T$. To optimize overall efficiency, a natural choice may be $L_\tau \sim 1/T$ when T is small. Finally, following each molecular dynamics trajectory, there is the MC accept/reject step. The acceptance probability $p_{\rm accept}$ vanishes rapidly with increasing N, with decreasing T, and with decreasing accuracy in the action estimate. The overall cost of the method scales by the associated factor $f_{\rm mc} = 1/p_{\rm accept}$. The complexity of hybrid MC makes direct comparison to our Langevin approach difficult. Both scale linearly with N (ignoring $f_{\rm mc}$) but hybrid MC appears to be less efficient at low temperatures, when accuracy requirements are high. Hybrid MC has the advantage that inertial dynamics may decrease the decorrelation time for sampling ϕ.

To demonstrate our method, we apply it to the triangular KL model defined by the Hamiltonian

$$\mathcal{H} = -\sum_{ij\sigma} t_{ij} c^\dagger_{i\sigma} c_{j\sigma} - J \sum_{j\mu\nu} \mathbf{S}_j \cdot c^\dagger_{j\mu} \boldsymbol{\sigma}_{\mu\nu} c_{j\nu}, \qquad (8)$$

where $c^\dagger_{j\sigma}(c_{j\sigma})$ is the creation (annihilation) operator of an electron with spin σ on site j, $\mathbf{S}_j$ is a classical Heisenberg spin with $|\mathbf{S}_j| = 1$, and $\boldsymbol{\sigma}_{\mu\nu} = (\sigma^x_{\mu\nu}, \sigma^y_{\mu\nu}, \sigma^z_{\mu\nu})$ is a vector of Pauli matrices. The dimensionless hopping coefficients are $t_{ij} = 1$ if i and j are nearest neighbor sites on the triangular lattice; $t_{ij} = 0$ otherwise.

By perfect nesting of the Fermi surface, it has been argued that the chiral $3q$ configuration [Fig. 1(c)] is the ground state at 3/4 electron filling fraction with small coupling.[17] This state is of special interest as it exhibits a spontaneous quantum Hall effect. Variational calculation on the 2×2 plaquette also predicts stability of the $3q$ state.[35] An unconstrained MC study of this phase at 3/4 filling has not been achieved due to severe numerical difficulties. Very low temperatures, $T \lesssim 0.001$, and small couplings, $J \lesssim 0.3$, are required to stabilize $3q$. A numerical method must be very accurate to resolve the small gap in the density of states (of width $\sim J^2$). Also, the $3q$ state is stabilized by a susceptibility which diverges as $(\log N)^2$,

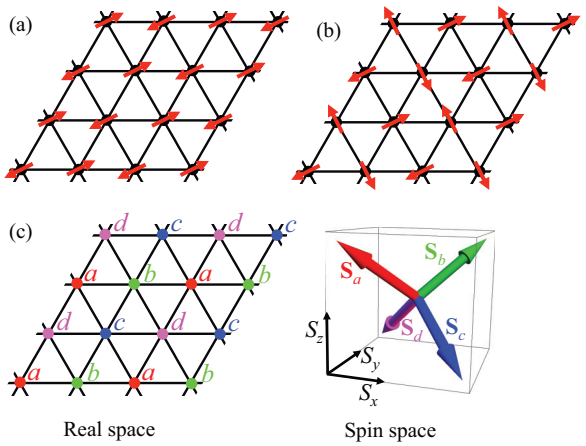

FIG. 1. (Color online) Three competing periodic 2×2 spin textures in the triangular KL model at 3/4 filling. The (a) $1q$, (b) $2q$, and (c) $3q$ phases are named according to their number of reciprocal lattice vectors. The $3q$ phase maximizes chirality $\chi = \mathbf{S}_i \times \mathbf{S}_j \cdot \mathbf{S}_k = \pm 4/3^{3/2}$ averaged over triangular plaquettes $[ijk]$ and yields a quantum Hall effect at 1/4 and 3/4 fillings. The $1q$ and $2q$ phases break rotational symmetry.

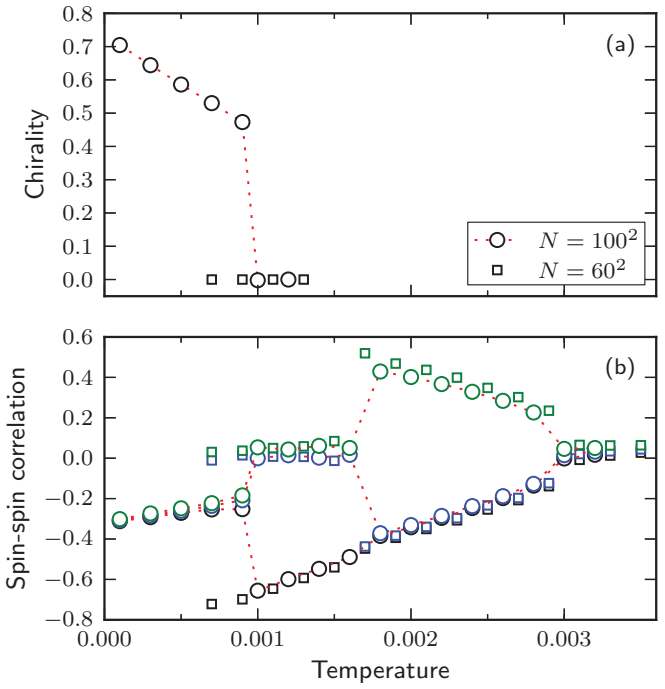

FIG. 2. (Color online) Phase diagram of the triangular KL model with $J = 0.2$ and $\mu = 1.947$, corresponding to filling fraction ~3/4. (a) At low temperatures the preferred $3q$ phase is identified by $\langle\chi\rangle \neq 0$. System size $N = 100^2$ (circles) is sufficient to stabilize the $3q$ phase, but $N = 60^2$ is not. (b) Spin-spin correlation functions $\langle \mathbf{S}_i \cdot \mathbf{S}_j \rangle$ for three nearest-neighbor orientations. Three first-order phase transitions are apparent: $3q \to 2q$ at $T = 0.0010$, $2q \to 1q$ at $T = 0.0017$, and $1q \to$ paramagnet at $T = 0.0029$.

so large lattice sizes are required ($N \approx 100^2$). Due to these challenges, this system offers a demanding test of our method.

We choose $J = 0.2$, $\mu = 1.947$, and $N = 100^2$. The three phases in Fig. 1 have similar energy densities: -4.15552, -4.15550, and -4.15525 for $3q$, $2q$, and $1q$, respectively. The ferromagnetic energy density, -4.15278, is not competitive. We use our method with $M = 1000$ and $z = 0.02$. At $M = 1000$, KPM estimates of energy differences are accurate to order 10^{-5}. With $z = 0.02$ the effective Langevin temperature is increased by $\Delta T_{\text{eff}} \approx 0.0002$.

In Fig. 2(a) we observe melting of the chiral $3q$ ground state. The mean chirality $\chi = \mathbf{S}_i \times \mathbf{S}_j \cdot \mathbf{S}_k$ of triangular plaquettes $[ijk]$ abruptly disappears at a first-order phase transition at $T \approx 0.0010$. This transition is not to a paramagnetic phase. To distinguish the phases $3q$, $2q$, and $1q$ we consider the (unordered) set of nearest-neighbor spin-spin correlations $C = \{\langle \mathbf{S}_\mathbf{x} \cdot \mathbf{S}_{\mathbf{x}+\langle 1,0\rangle}\rangle, \langle \mathbf{S}_\mathbf{x} \cdot \mathbf{S}_{\mathbf{x}+\langle 1,\sqrt{3}\rangle/2}\rangle, \langle \mathbf{S}_\mathbf{x} \cdot \mathbf{S}_{\mathbf{x}+\langle -1,\sqrt{3}\rangle/2}\rangle\}$, averaged over lattice sites $\mathbf{x}$. Pure $3q$, $2q$, and $1q$ phases yield $C_{3q} = \{-1/3, -1/3, -1/3\}$, $C_{2q} = \{0, 0, -1\}$, and $C_{1q} = \{-1, -1, 1\}$. The latter two states break rotational symmetry of the triangular lattice.

Figure 2(b) shows the three elements of C as a function of T. At $T = 0$ we find $C = C_{3q}$ as expected. We observe *three* first-order transitions at $T = 0.0010$, 0.0017, and 0.0029 to the $2q$, $1q$, and paramagnetic phases, respectively. The $2q$ phase is identified by its correlation set C, which has two zero elements and one negative element. In the $1q$ phase, C has one positive element and two negative (symmetric) elements. To avoid equilibration issues, we use initial conditions with explicitly broken chiral symmetry, $\langle \chi \rangle > 0$.

We now discuss the dynamical, nonequilibrium process by which $3q$ chiral symmetry breaking occurs at low temperatures. We use our method to study the phase ordering kinetics of chiral domains following a quench from infinite to zero temperature. In the spirit of time-dependent Ginzburg-Landau (Model A[36]) for phase ordering, we expect our overdamped Langevin dynamics to capture the qualitative large-scale aspects of chiral domain growth and defect evolution.[37] Our Langevin dynamics can be viewed as the overdamped limit of the Landau-Lifshitz-Gilbert equation (to which our KPM-based force estimates may also be applied[38]). We find interesting features not usually present in Model A systems, consistent with effective long-range, many-body interactions in the KL models studied.

We first consider $\sim 1/4$ filling with $J = 3$ and $\mu = -3.2$. Previous work found a robust $3q$ phase with $N \leqslant 16^2$.[18] We

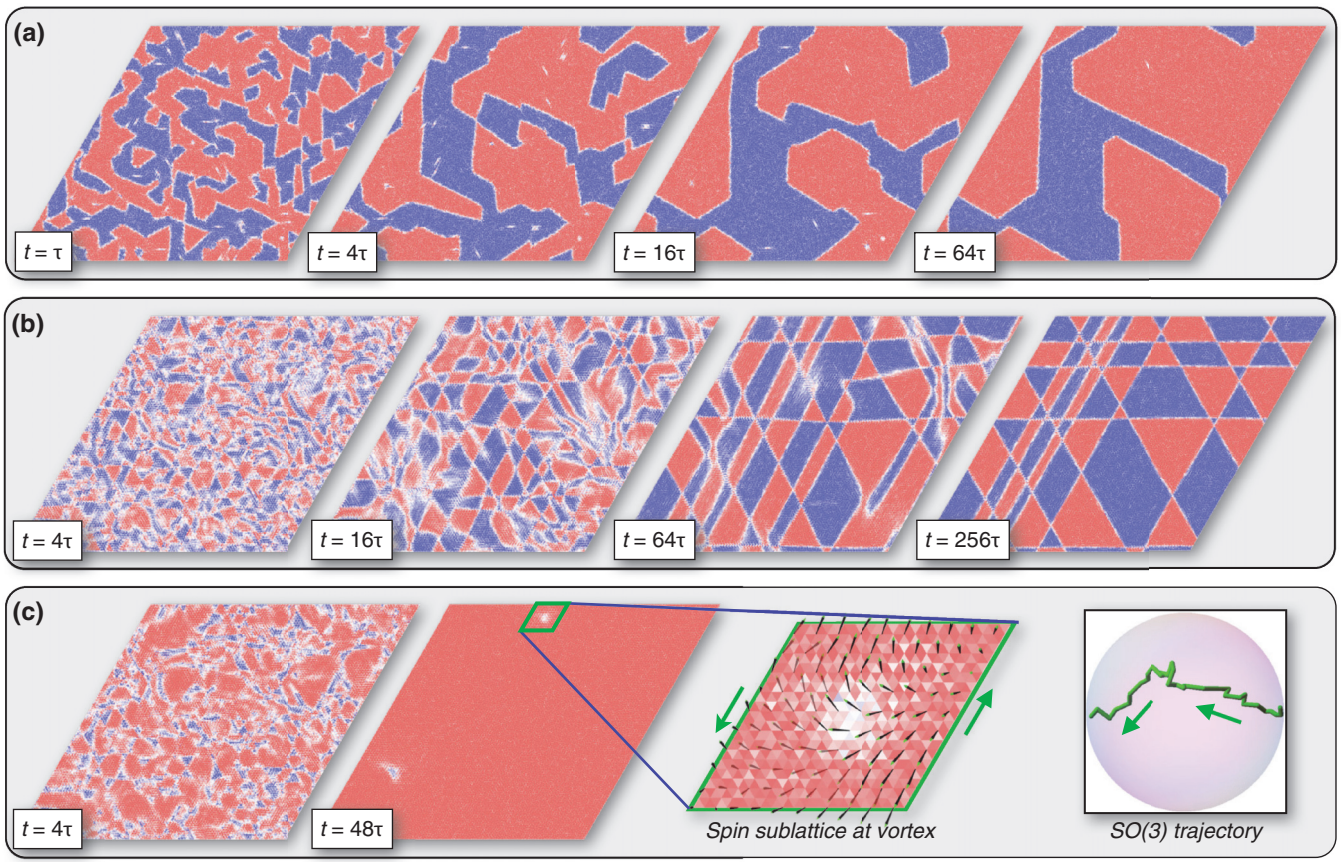

FIG. 3. (Color online) Phase ordering in the 200×200 triangular KL model after a quench from $T = \infty$ to $T = 0$. The color gradient, ranging from red to blue, is the local chirality. Langevin time is in units of $\tau = 1.28 \times 10^4$. (a) $J = 3$, $\mu = -3.2$ ($\sim 1/4$ filling). Domain coarsening with strong anisotropy is observed. $\mathbb{Z}_2$ vortices (white dots) rapidly annihilate each other. (b) $J = 0.2$, $\mu = 1.947$ ($\sim 3/4$ filling). The system is trapped in a complex metastable state. (c) $J = 0.2$, $\mu = 1.947$, $B_z = 8\pi/\sqrt{3N}$ ($\sim 3/4$ filling). An external field breaks chiral symmetry, and the system rapidly evolves to the $3q$ ground state. A $\mathbb{Z}_2$ vortex is identified by the winding of a Burger's circuit (green) in $SO(3)$ space, a filled projective sphere in the axis-angle representation. A $\mathbb{Z}_2$ vortex is enlarged in the third panel.

use our approach to study the ordering dynamics at $N = 200^2$ with $M = 500$ and $z = 0.005$. Figure 3(a) shows the evolution of chirality ranging from red (positive) to blue (negative). The coarsening of chiral domains is analogous to what is observed in Model A, but we observe strong anisotropy of domain walls. The dynamics slows at large times, consistent with a characteristic length scale that grows as $\ell \sim t^{1/2}$.[39]

The ordering dynamics for $\sim 3/4$ filling with $J = 0.2$, $\mu = 1.947$, $M = 500$, and $z = 0.02$ is shown in Fig. 3(b). Surprisingly, the system now evolves into a long lived metastable state with remarkable chiral domain wall patterns. The system can be annealed to the pure $3q$ phase by raising temperature, but experimentally it is easier to explicitly break chiral symmetry with an applied external magnetic field B_z.[19] We introduce orbital coupling into Eq. (8) by applying a nonuniform phase $\theta_{ij} = B_z \hat{z} \cdot \mathbf{x}_i \times \mathbf{x}_j / 2$ to the hopping coefficients $t_{ij} = e^{-i\theta_{ij}}$, with $\mathbf{x}_i$ the position of lattice site i. The smallest magnetic field consistent with periodic boundaries, $B_z = 8\pi/\sqrt{3N}$, causes the system to rapidly reach the uniform chiral $3q$ phase [see Fig. 3(c)].

The small white dots visible in Fig. 3(a) are topological defects associated with $\mathbb{Z}_2$ winding of the $SO(3)$ manifold, and are predicted to have fractional charge.[40] A $\mathbb{Z}_2$ vortex is enlarged in Fig. 3(c). One of the four $3q$ spin sublattices is shown. We can understand this defect by constructing a closed Burger's circuit (in green) that encircles it. The Burger's circuit corresponds to a trajectory in $SO(3)$ space which, in the axis-angle representation, is a filled sphere with antipodal points identified. This Burger's circuit has winding number 1 because it wraps $SO(3)$. The vortex is $\mathbb{Z}_2$ because the only homotopically distinct winding numbers are 0 and 1. Consequently, any pair of $\mathbb{Z}_2$ vortices may annihilate. In the evolution shown in Fig. 3(a), we observe many vortices annihilating with each other and with domain walls.

In summary, we have introduced a highly accurate and efficient numerical method to study the broad class of Hamiltonians that couple fermions to classical degrees of freedom. Our method enables the study of complex systems of unprecedented size. In the triangular KL model at 3/4 filling, we required lattice sizes $N \geqslant 100^2$ and six digits of precision to resolve logarithmic divergences that give rise to an anomalous Hall effect. Large system sizes also allow us to bridge the gap between quantum and mesoscopic physics. For $N = 200^2$ we are able to probe chiral domain dynamics, metastable trapping, and $\mathbb{Z}_2$ vortex dynamics that would be inaccessible with standard approaches.

We thank Ivar Martin and Cristian Batista for useful discussions. This work was carried out under the auspices of the NNSA of the U.S. DOE at LANL under Contract No. DE-AC52-06NA25396 and supported by the LANL/LDRD Program. The calculations were performed using the CCS-7 Darwin cluster.

*kbarros@lanl.gov

[1] S. Doniach, Physica B & C **91B**, 231 (1977).
[2] L. M. Falicov and J. C. Kimball, Phys. Rev. Lett. **22**, 997 (1969).
[3] P. G. De Gennes, *Superconductivity of Metals and Alloys* (Benjamin, New York, 1966).
[4] R. Blankenbecler, D. J. Scalapino, and R. L. Sugar, Phys. Rev. D **24**, 2278 (1981).
[5] J. E. Hirsch and R. M. Fye, Phys. Rev. Lett. **56**, 2521 (1986).
[6] J. L. Alonso, L. A. Fernández, F. Guinea, V. Laliena, and V. Martín-Mayor, Nucl. Phys. B **596**, 587 (2001).
[7] N. Furukawa, Y. Motome, and H. Nakata, Comput. Phys. Commun. **142**, 410 (2001).
[8] N. Furukawa and Y. Motome, J. Phys. Soc. Jpn. **73**, 1482 (2004).
[9] G. Alvarez, C. Şen, N. Furukawa, Y. Motome, and E. Dagotto, Comput. Phys. Commun. **168**, 32 (2005).
[10] G. Alvarez, P. K. V. V. Nukala, and E. D'Azevedo, J. Stat. Mech. (2007) P08007.
[11] A. Weiße, Phys. Rev. Lett. **102**, 150604 (2009).
[12] G. H. Jonker and J. H. Van Santen, Physica **16**, 337 (1950).
[13] A. P. Ramirez, J. Phys.: Condens. Matter **9**, 8171 (1997).
[14] E. Dagotto, T. Hotta, and A. Moreo, Phys. Rep. **344**, 1 (2001).
[15] X. Z. Yu, Y. Onose, N. Kanazawa, J. H. Park, J. H. Han, Y. Matsui, N. Nagaosa, and Y. Tokura, Nature (London) **465**, 901 (2010).
[16] D. Solenov, D. Mozyrsky, and I. Martin, Phys. Rev. Lett. **108**, 096403 (2012).
[17] I. Martin and C. D. Batista, Phys. Rev. Lett. **101**, 156402 (2008).
[18] Y. Kato, I. Martin, and C. D. Batista, Phys. Rev. Lett. **105**, 266405 (2010).
[19] Y. Machida, S. Nakatsuji, S. Onoda, T. Tayama, and T. Sakakibara, Nature (London) **463**, 210 (2010).
[20] B. G. Ueland, C. F. Miclea, Y. Kato, O. Ayala-Valenzuela, R. D. McDonald, R. Okazaki, P. H. Tobash, M. A. Torrez, F. Ronning, R. Movshovich, Z. Fisk, E. D. Bauer, I. Martin, and J. D. Thompson, Nat. Commun. **3**, 1067 (2012).
[21] A. Griewank, in *Mathematical Programming: Recent Developments and Applications*, edited by M. Iri and K. Tanabe (Kluwer Academic, Dordrecht, The Netherlands, 1989), pp. 83–108.
[22] R. N. Silver and H. Röder, Int. J. Mod. Phys. C **5**, 735 (1994).
[23] A. Weiße, G. Wellein, A. Alvermann, and H. Fehske, Rev. Mod. Phys. **78**, 275 (2006).
[24] L.-W. Wang, Phys. Rev. B **49**, 10154 (1994).
[25] D. Jackson, Ph.D. thesis, Georg-August-Universität Göttingen, 1911.
[26] D. Jackson, Trans. Am. Math. Soc. **13**, 491 (1912).
[27] *Handbook of Mathematical Functions*, edited by M. Abramowitz and I. A. Stegun (Dover, New York, 1972).
[28] T. Iitaka and T. Ebisuzaki, Phys. Rev. E **69**, 057701 (2004).
[29] A. F. Voter, J. D. Kress, and R. N. Silver, Phys. Rev. B **53**, 12733 (1996).
[30] G. H. Golub and C. F. van Loan, *Matrix Computations*, 3rd ed. (Johns Hopkins University Press, Baltimore, MD, 1996).
[31] A. P. Sutton, M. W. Finnis, D. G. Pettifor, and Y. Ohta, J. Phys. C **21**, 35 (1988).
[32] In the particular case of tight-binding molecular dynamics, the forces are often effectively local and the single particle Hamiltonian may be truncated. After this truncation, the method in Ref. 29 scales linearly with system size N.

[33]R. T. Scalettar, D. J. Scalapino, and R. L. Sugar, Phys. Rev. B **34**, 7911 (1986).
[34]S. Duane, A. Kennedy, B. J. Pendleton, and D. Roweth, Phys. Lett. B **195**, 216 (1987).
[35]Y. Akagi and Y. Motome, J. Phys. Soc. Jpn. **79**, 083711 (2010).
[36]P. C. Hohenberg and B. I. Halperin, Rev. Mod. Phys. **49**, 435 (1977).
[37]P. Chaikin and T. Lubensky, *Principles of Condensed Matter Physics* (Cambridge University Press, Cambridge, 1995).
[38]B. Skubic, J. Hellsvik, L. Nordström, and O. Eriksson, J. Phys.: Condens. Matter **20**, 315203 (2008).
[39]A. J. Bray, Adv. Phys. **43**, 357 (1994).
[40]A. Rahmani, R. A. Muniz, and I. Martin, Phys. Rev. X **3**, 031008 (2013).